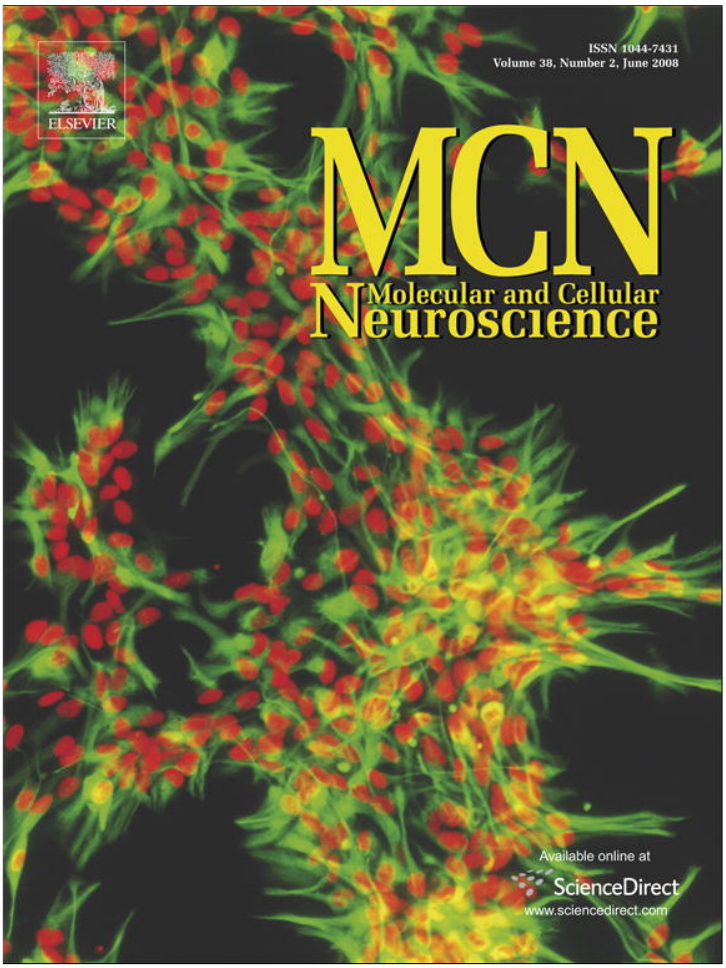

ELSEVIER

MCN Molecular and Cellular Neuroscience

www.elsevier.com/locate/ymcne
Mol. Cell. Neurosci. 38 (2008) 266–276

Synaptopodin maintains the neural activity-dependent enlargement of dendritic spines in hippocampal neurons

Reiko Okubo-Suzuki,[a,b] Daisuke Okada,[a,c] Mariko Sekiguchi,[a,c] and Kaoru Inokuchi[a,b,c,*]

[a]*Mitsubishi Kagaku Institute of Life Sciences, MITILS, 11 Minamiooya, Machida, Tokyo 194-8511, Japan*
[b]*Graduate School of Environment and Information Sciences, Yokohama National University, Yokohama, Kanagawa 240-8511, Japan*
[c]*Japan Science and Technology Agency, CREST, Kawaguchi, Saitama 332-0012, Japan*

Received 11 October 2007; revised 25 February 2008; accepted 1 March 2008
Available online 14 March 2008

Synaptopodin (SYNPO) is an F-actin interacting protein expressed in dendritic spines and upregulated during the late-phase of long-term potentiation. Here, we investigated whether SYNPO regulates spine morphology through interactions with F-actin, the major cytoskeletal element of spines. In primary hippocampal neuron cultures, both endogenous and exogenous SYNPO localized preferentially in large spines under basal conditions. SYNPO overexpression did not affect the number or volume of spines in unstimulated neurons. Pharmacological activation of synaptic NMDA receptors transiently increased spine volume in control neurons, while the increase was persistent in neurons overexpressing SYNPO. In addition, exogenous SYNPO in PtK2 cells suppressed staurosporine-dependent disruption of F-actin stress fibers, suggesting that SYNPO protected F-actin from disruption. These results suggest that SYNPO stabilized activity-dependent increases in spine volume and imply that late-phase changes in spine morphology involve SYNPO.

Introduction

Synaptopodin (SYNPO) is an actin-associated protein in the dendritic spines of telencephalic neurons and renal podocytes (Mundel et al., 1997). SYNPO elongates and bundles F-actin through interactions with α-actinin in HEK293 cells (Asanuma et al., 2005), and induces stress fiber formation in podocytes by regulating RhoA signaling (Asanuma et al., 2006). We have previously identified the SYNPO gene among several genes upregulated *in vivo* during long-term potentiation (LTP) (Inokuchi et al., 1996a,b; Kato et al., 1997; Matsuo et al., 1998, 2000). When LTP is induced at perforant path-granule cell synapses in the dentate gyrus, SYNPO mRNA is upregulated in the granule cell soma and protein levels increase in the activated synaptic layer (Fukazawa et al., 2003; Yamazaki et al., 2001). SYNPO is localized in dendritic spines, especially on the spine apparatus (Deller et al., 2000). SYNPO-deficient mice lack the spine apparatus and show impairment in both the early and late phases of LTP (E- and L-LTP) (Deller et al., 2003). Thus, SYNPO is involved in, and induced during, protein-synthesis-dependent L-LTP. However, the function of SYNPO in neurons is still unknown. We have previously shown that L-LTP is accompanied *in vivo* by an increase in F-actin in the activated synaptic layer, and that inhibition of actin polymerization impairs L-LTP (Fukazawa et al., 2003). Therefore, L-LTP may be associated with a persistent increase in spine volume and F-actin accumulation.

In this study, we investigated whether SYNPO regulates spine morphology, by expressing SYNPO tagged with enhanced green fluorescent protein (SE) in primary cultures of hippocampal neurons. We found that SYNPO was preferentially localized in large spines and that SYNPO did not affect static spine morphology. Pharmacological activation of synaptic NMDA receptors only transiently increased spine volume in control neurons, while the increase was persistent in SYNPO overexpressing neurons. We also observed that ectopic expression of SYNPO in PtK2 cells counteracted the staurosporine-dependent disruption of F-actin, suggesting that SYNPO protects F-actin from disruption. These results suggest that SYNPO maintains the activity-dependent increase in spine volume, and imply that the late-phase changes in spine morphology involve SYNPO.

Results

Splicing variants of SYNPO in the rat hippocampus

There are three known splice variants of mouse synaptopodin (SYNPO) mRNA, Synpo-short, Synpo-long and Synpo-T (Fig. 1A). Synpo-short is expressed in neurons, while the other

* Corresponding author. Mitsubishi Kagaku Institute of Life Science, MITILS, 11 Minamiooya, Machida, Tokyo 194-8511, Japan. Fax: +81 42 724 6318.
E-mail address: kaoru@mitils.jp (K. Inokuchi).
Available online on ScienceDirect (www.sciencedirect.com).

1044-7431/$ - see front matter © 2008 Elsevier Inc. All rights reserved.
doi:10.1016/j.mcn.2008.03.001

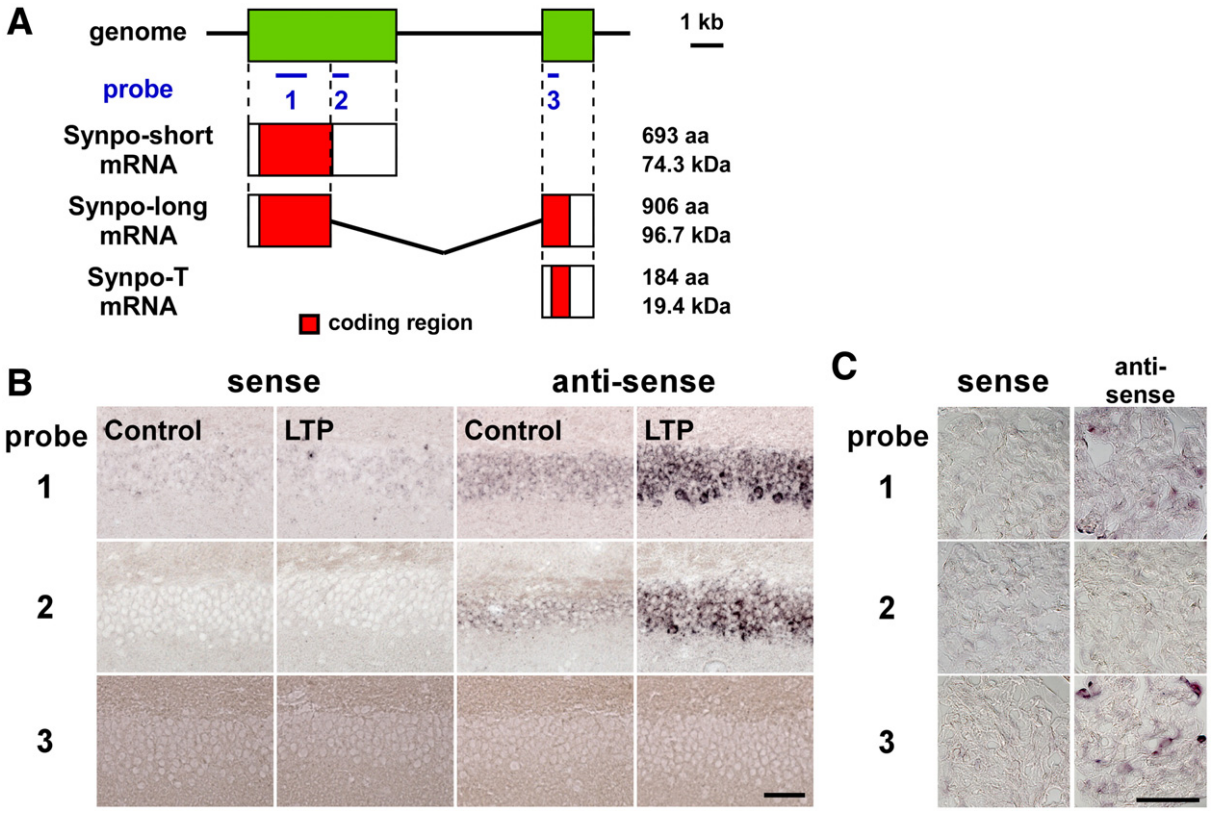

Fig. 1. Rat hippocampal expression of Synpo-short mRNA and upregulation during LTP. (A) Genomic organization and alternative splice products of rat SYNPO. The three probes for *in situ* hybridization are indicated by blue lines. Exons are indicated by green boxes. The number of amino acids (aa) and the putative molecular weight (kDa) of each protein is shown to the right. (B) Representative *in situ* hybridization photographs of the granule cell layer of the dentate gyrus. Brains were dissected 3 h after the delivery of high frequency stimulation (LTP). The contralateral dentate gyrus served as a control (control). Scale bar, 50 μm. Note that probe 3 gave no signal. (C) Representative *in situ* hybridization photographs of rat kidney glomeruli. Scale bar, 50 μm. Note that probe 2 gave no signal.

variants are exclusively expressed in the kidney (Asanuma et al., 2005). Using *in situ* hybridization, we confirmed that only Synpo-short was expressed in the dentate gyrus of the rat hippocampus (Fig. 1B), and that Synpo-long and/or Synpo-T were expressed in glomeruli of the rat kidney (Fig. 1C). We also found that LTP increased the expression level of Synpo-short in the dentate gyrus *in vivo* (Fig. 1B).

Next, we confirmed that the endogenous SYNPO protein in the hippocampus is Synpo-short. The neuronal SYNPO protein exhibits an apparent molecular mass of 100 kDa on SDS-PAGE gels (Mundel et al., 1997). Western blots probed with an antibody against SYNPO showed an endogenous 100 kDa protein in the hippocampus (Fig. 2). The mobility of the protein is almost identical to ectopically expressed Myc-tagged Synpo-short in HEK293T cells (Fig. 2). EGFP-fused Synpo-short and Myc-tagged Synpo-long had molecular masses of 125 kDa (Fig. 2). These results indicate that Synpo-short is the major splice variant of SYNPO expressed in the hippocampus. Therefore, we used Synpo-short to examine the role of SYNPO in spine morphology.

Correlation between SYNPO localization and spine volume

SYNPO has been localized in dendritic spines (Deller et al., 2000; Mundel et al., 1997). We noticed, however, that the SYNPO expression level differed among spines, regardless of whether SYNPO was endogenously or exogenously expressed. We tested the hypothesis that the heterogeneous pattern of SYNPO expression is a consequence of SYNPO function.

We first examined whether the distribution of SYNPO is correlated with that of F-actin in spines under basal conditions. Primary hippocampal neurons cultured at low density were double stained with anti-SYNPO antibody and TRITC-phalloidin (Fig. 3A). Intense F-actin staining was detected in spines with high levels of endogenous SYNPO. SYNPO immunoreactivity in spines positively correlated with phalloidin staining (Fig. 3B; $r=0.77$; $n=255$ spines from one neuron). Similar correlations were observed in other neurons examined ($0.56 \leq r \leq 0.88$; 10 neurons, 109–255 spines per neuron).

Because F-actin is the major cytoskeletal element in spines, the F-actin levels may influence the spine volume. Given the correlation between SYNPO and F-actin in spines (Fig. 3B), we predicted that the levels of SYNPO protein would also correlate with spine volume. Primary hippocampal neurons cultured at high density were transfected after culturing 9 days in vitro (DIV) with SYNPO (Synpo-short)-EGFP (SE) and DsRed2, as a marker for spine volume (Fig. 3C). We measured the fluorescence intensities of both SE and DsRed2 in spines on 21–27 DIV. The SE content in spines strongly correlated with DsRed2 fluorescence intensity (Fig. 3D; $r=0.78$; $n=126$ spines from one neuron). Similar correlations were observed in other neurons ($0.65 \leq r \leq 0.93$; 15 neurons, 67–237 spines per neuron). Thus, the SYNPO protein levels in spines were positively correlated with spine volume.

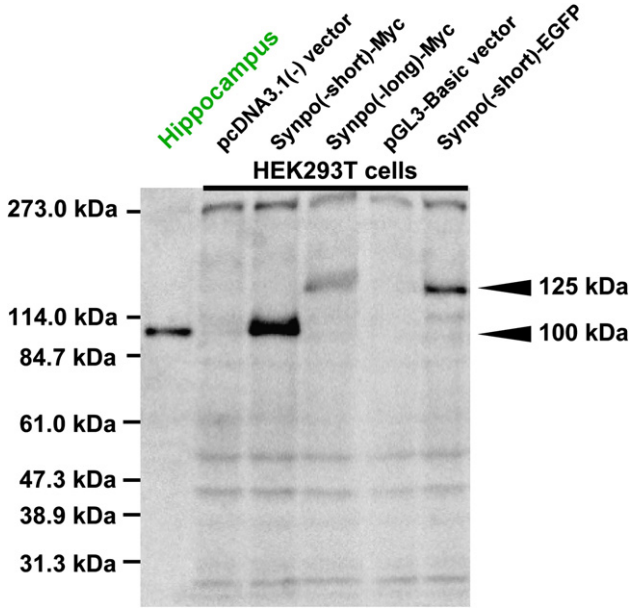

Fig. 2. Apparent molecular mass of Synpo (short)-Myc and Synpo (short)-EGFP. HEK293T cells were transfected with Synpo(-short)-Myc, Synpo(-long)-Myc, or Synpo(-short)-EGFP. The pcDNA3.1(−) and pGL3-Basic vectors were transfected as controls. The Synpo(-short)-Myc protein and the endogenous SYNPO protein from the hippocampus had identical molecular masses of 100 kDa. The molecular masses of Synpo(-short)-EGFP and Synpo(-long)-Myc, approximately 125 kDa, were larger than that of Synpo(-short)-Myc.

We examined whether endogenous SYNPO also localized in larger spines. Neurons cultured at high density were transfected at 9 DIV with EGFP for visualization of cell morphology, and were then stained with an anti-SYNPO antibody on 21–27 DIV. We classified spines according to the presence of SYNPO immunoreactivity, and then measured their projection area, as indicated by EGFP fluorescence. Areas of SYNPO immunoreactive spines (0.63 ± 0.04 μm^2, $n=20$ neurons, 8–71 spines per neuron) were significantly larger than the areas of spines lacking SYNPO (0.44 ± 0.03 μm^2, $n=20$ neurons, 28–168 spines per neuron, $p<0.001$). These results suggest that the endogenous SYNPO expression level was higher in larger spines. Furthermore, these results are consistent with previous findings that SYNPO localizes to the spine apparatus (Deller et al., 2000) and that the spine apparatus localizes to large spines (Spacek and Harris, 1997). Taken together, our results suggested that both endogenous and exogenous SYNPO were preferentially localized in large spines under basal conditions.

SYNPO does not affect the number and size of spines

Primary cultures of hippocampal neurons on 9 DIV were co-transfected with SE or EGFP (as a control) and DsRed2, to examine whether overexpression of SYNPO influences the number and/or size of dendritic spines. Neurons on 21 DIV were stained with an anti-SYNPO antibody to examine the level of SYNPO expression (Fig. 4A). We counted the number of spines and measured the projection area of spines in both EGFP- and SE-expressing cells. The number of spines in a 10-μm-dendritic region was not significantly different between EGFP- and SE-expressing cells (Fig. 4B; EGFP, 4.2 ± 0.57, $n=5$ neurons; SE, 4.7 ± 0.93, $n=5$ neurons; $p=0.65$). The spine areas were also not significantly different between these neuronal populations (Fig. 4C; EGFP, 0.90 ± 0.04 μm^2, $n=5$ neurons; SE, 0.98 ± 0.06 μm^2, $n=5$ neurons; $p=0.33$). SYNPO immunoreactivity was significantly increased in spines of SE-expressing cells compared to EGFP-expressing cells (Fig. 4D; EGFP, 1.0 ± 0.15 fold, $n=5$ neurons; SE, 3.1 ± 0.57 fold, $n=5$ neurons; $p<0.01$), excluding the possibility that these results are due to a failure to overexpress SYNPO. Thus, SYNPO overexpression did not affect the number or size of spines.

SYNPO does not affect the evoked changes in spine size during the early phase

Spine size is affected by neural activity, particularly activity evoking LTP (Matsuzaki et al., 2004). We next examined whether SYNPO affects neural activity-dependent changes in spine size using time-lapse confocal microscopy. To examine the effect of SYNPO overexpression on spine volume, 9 DIV neurons were co-transfected with SE or EGFP and DsRed2. To evoke spine size changes associated with LTP, we pharmacologically activated synaptic NMDA receptors by bath perfusion of Mg^{2+}-free ACSF containing 10 μM glycine and 3 μM picrotoxin. Neurons in culture make synaptic connections where glutamatergic transmission takes place spontaneously. The GABA-A receptor inhibitor, picrotoxin, suppresses inhibitory transmission in the network, thereby raising the frequency and probability of excitatory transmission (Hardingham et al., 2002). Extracellular Mg^{2+}-free ACSF releases the Mg^{2+} blockade of NMDA receptor channels and glutamate released from presynaptic terminals together with the co-agonist, glycine, activate NMDA receptors synaptically. This method for stimulation is similar to ones that evoke chemical LTP (Lu et al., 2001; Otmakhov et al., 2004).

The DsRed2 fluorescence in both SE- and EGFP-expressing neurons 15 min after stimulation was variable. DsRed2 fluorescence increased in some spines, whereas it was reduced or unchanged in others (Figs. 5A–C). This heterogeneity arises from the fact that the effects of our stimulation method depend on the intrinsic activity of presynaptic fibers. Thus, we pooled data from several cells for statistical analysis. To compare changes among different cells, the fold change in intensity relative to the pre-stimulus average in each spine was calculated. To see both transient and long lasting effects from the stimuli, images were taken at early (15, 30, and 45 min after the stimulus onset) and late (450, 465 and 480 min) stages.

In the early stage, spines with a smaller initial volume grew more following stimulation (Fig. 5B), however, overexpression of SYNPO had no effect on changes in spine size. The average fold change in DsRed2 fluorescence was 1.23 ± 0.02 ($n=1257$ spines on 9 neurons) for SE-expressing neurons and 1.19 ± 0.02 ($n=1218$ spines on 8 neurons) for EGFP-expressing neurons ($p=0.12$) (Fig. 5D). Frequency distribution plots (Fig. 5C) show that some spine populations responded more dramatically, but overexpression of SYNPO did not influence these changes. For example, DsRed2 fluorescence in $10.2 \pm 2.5\%$ of EGFP-expressing spines and $9.0 \pm 2.6\%$ of SE-expressing spines was doubled (EGFP, $n=8$ neurons; SE, $n=9$ neurons; $p=0.76$) (Figs. 5C, E). Similarly, DsRed2 fluorescence in $3.7 \pm 1.4\%$ of EGFP-expressing spines and $4.0 \pm 1.5\%$ of SE-expressing spines was reduced by at least half ($p=0.91$) (Figs. 5C, F). These changes depended on the presence of the stimuli, because spine volume did not change significantly in the absence of the stimuli (Figs. 5C, E, F). These results indicate that overexpression of SYNPO has no effect on changes in spine volume during the early stage.

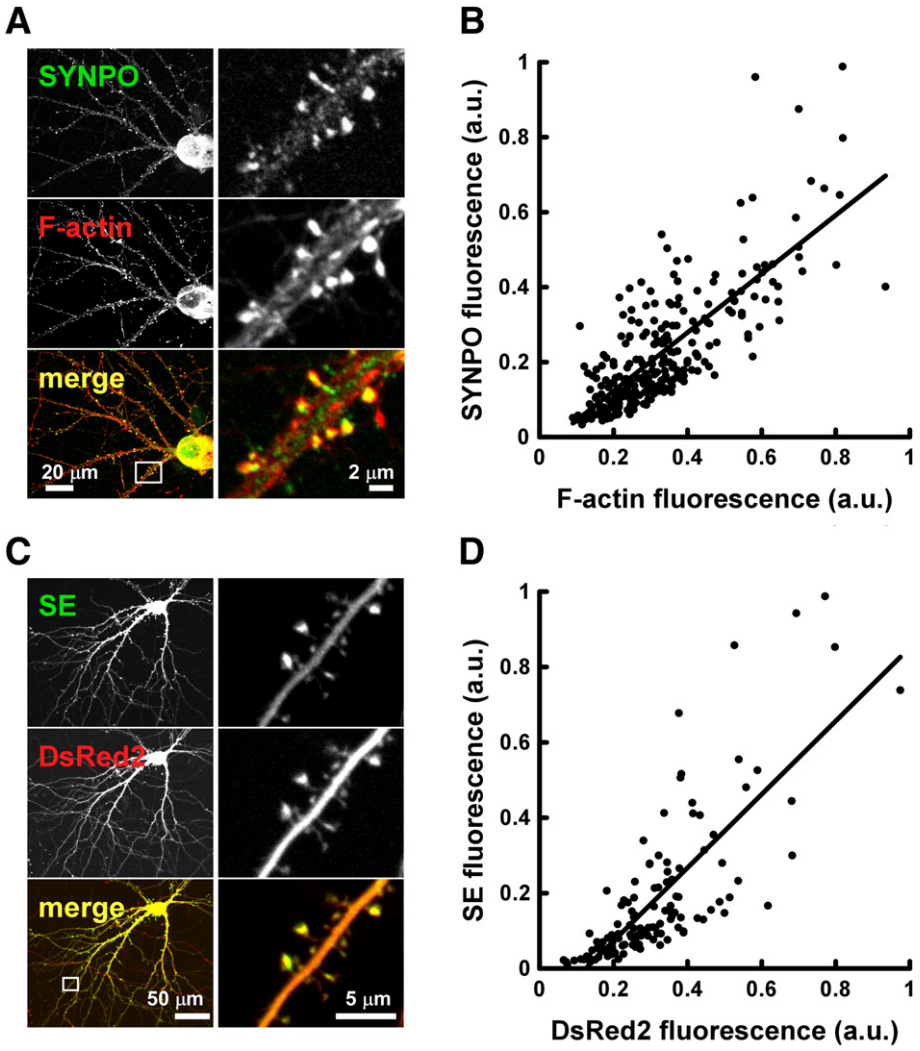

Fig. 3. Correlation between SYNPO expression in spines and F-actin intensity (A and B) or spine volume (C and D). (A) Hippocampal neurons in dissociated cultures were immunolabeled on 21 DIV with an anti-SYNPO antibody (top panel, and green in the bottom panel) and stained with TRITC-phalloidin (middle panel, and red in the bottom panel). (B) SYNPO immunoreactivity positively correlated with phalloidin intensity. (C) Dissociated hippocampal cultures were co-transfected with SYNPO-EGFP (top panel, and green in the bottom panel) and DsRed2 (middle panel, and red in the bottom panel) on 9 DIV, and imaged on 23 DIV. (D) The fluorescence intensity of DsRed2 positively correlated with SYNPO-EGFP staining. Boxes in (A) and (C) indicate regions of higher magnification shown in the right panels. a.u., arbitrary unit.

SYNPO overexpression maintains the evoked spine enlargement in late stage

SYNPO is upregulated several hours after L-LTP induction (Yamazaki et al., 2001). We therefore examined whether SYNPO is involved in maintenance of the enlarged spine volume in the late stage rather than the stimulus-dependent transient changes in the early stage. We analyzed the late-stage changes in DsRed2 fluorescence of spines whose size in the early stage had either increased at least two fold or decreased by half (Figs. 6A, D).

The average fold-increase in DsRed2 fluorescence in SE-expressing spines was 2.49±0.05 in the early stage and 2.50±0.13 in the late stage ($p=0.85$), indicating that the enlarged spine volume of SE-expressing neurons was maintained through the late stage (Fig. 6B). In contrast, DsRed2 fluorescence in EGFP-expressing spines increased transiently (2.57±0.04 fold) and was reduced significantly in the late stage (1.95±0.07 fold; $p<0.001$) (Fig. 6B). These data indicate that the increase in DsRed2 fluorescence in both SE- and EGFP-expressing spines was similar ($p=0.14$) in the early stage but differed significantly in the late stage ($p<0.001$). In addition, the DsRed2 fluorescence ratio (R_{late}/R_{early}) of SE-expressing spines was 1.01±0.05, which was significantly different from EGFP-expressing spines (0.77±0.03; $p<0.001$).

The spines of both EGFP- and SE-expressing neurons that lost volume in the early stage regained their original size in the late stage (Figs. 6D–F). The average fold change in DsRed2 fluorescence of EGFP-expressing spines was 0.44±0.01 in the early stage and 1.13±0.11 in the late stage ($p<0.001$), while that of SE-expressing spines was 0.43±0.01 in the early stage and 0.95±0.07 in the late stage ($p<0.001$) (Fig. 6E). The DsRed2 fluorescence intensity in the late stage was not significantly different from the pre-stimulus fluorescence level (EGFP, $p=0.26$, SE, $p=0.53$) (Fig. 6E). The changes in DsRed2 fluorescence for EGFP- and SE-expressing spines were similar for both phases (early, $p=0.23$; late, $p=0.19$).

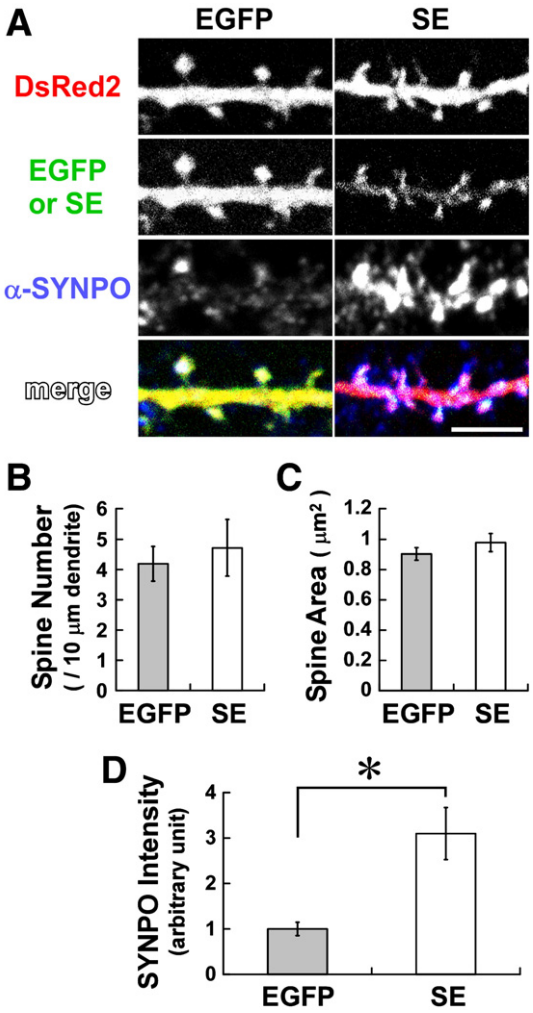

Fig. 4. The overexpression of SYNPO does not affect the density and area of spines. (A) Hippocampal cultures on 9 DIV were co-transfected with DsRed2 and SYNPO-EGFP (SE) or EGFP (control). The neurons were immunolabeled with anti-SYNPO on 21 DIV (α-SYNPO). Scale bar, 5 μm. (B) The numbers of spines in a 10 μm dendritic region of SE- and EGFP-expressing neurons are statistically indistinguishable. (C) The spine area of SE-expressing and control neurons are also statistically indistinguishable. (D) SYNPO immunoreactivity in spines of SE- and EGFP-expressing neurons. Values in (B,C, and D) are mean±SEM. Asterisk denotes $p<0.01$ (*t*-test).

Both EGFP- and SE-expressing spines had similar increases in the DsRed2 fluorescence ratio between the early and late stages (R_{late}/R_{early}, EGFP, 2.57±0.26; SE, 2.21±0.15; $p=0.23$) (Fig. 6F).

These results indicate that SYNPO maintains the pharmacological stimulus-evoked enlargement in spine volume up to 8 h, but it does not affect recovery in size of those spines that lost volume in the early stage.

SYNPO is concentrated in enlarged spines

We next examined the changes in SE fluorescence in order to determine whether SYNPO is actively recruited into spines (Fig. 7). We found that there is a positive correlation between SE and DsRed2 fluorescence in both early ($r=0.87$) (Fig. 7B) and late ($r=0.86$) (Fig. 7C) stages ($n=1257$ spines on 9 neurons). Therefore, the SE content was proportional to the spine volume when the spines were analyzed collectively, suggesting that the mechanism mediating spine enlargement also governs SE entry into the spines.

We then analyzed the subpopulations of spines that were either enlarged or reduced in volume in the early stage. SE fluorescence intensity in the enlarged spines increased in the late stage (early, 2.22±0.08; late, 2.65±0.21; $p<0.05$) (Figs. 7D, E), while the DsRed2 fluorescence in these spines remained constant (Figs. 6A–C). Therefore, SE in the enlarged spines increased more than expected from the increase in volume alone. In contrast, the EGFP fluorescence intensity in the enlarged spines of control neurons decreased in the late stage (early, 2.22±0.04; late, 1.71±0.06; $p<0.001$) (Fig. 7E) at a rate similar to that of the DsRed2 fluorescence (Figs. 6A–C), indicating that the EGFP levels were determined by spine volume. These results suggest that an active mechanism exists by which SYNPO is specifically targeted to enlarged spines independently of spine volume changes.

In contrast, the fold change in the SE and EGFP fluorescence intensities in the spines that lost volume in the early stage returned to pre-stimulus levels in the late stage (EGFP; early, 0.45±0.01; late, 0.99±0.10; $p<0.001$; SE; early, 0.47±0.02; late, 0.91±0.09; $p<0.001$) (Figs. 7F, G), as previously observed for DsRed2 fluorescence (Figs. 6D–F).

Synaptopodin suppresses the collapse of F-actin in PtK2 cells

We examined whether ectopic expression of SYNPO affected the maintenance of stress fibers in PtK2 cells (Fig. 8). PtK2 cells are large, flat epithelial cells whose cytoskeletal processes are easily observed and express virtually no endogenous SYNPO (data not shown). PtK2 cells were transfected with SE or EGFP (control), and were stained with TRITC-phalloidin. We observed that SE localized on stress fibers, especially at focal contacts (Fig. 8B), as has been previously shown for endogenous SYNPO in differentiated podocytes (Asanuma et al., 2006), and that EGFP was diffusely distributed in the cells (Fig. 8A).

PtK2 cells were treated with staurosporine, a Ser/Thr kinase inhibitor that is known to disrupt stress fibers in several cell types, including PtK2 cells (Hedberg et al., 1990). Treatment of cells with 100 nM staurosporine for 20 min led to a loss of stress fibers as previously described (Hedberg et al., 1990), and fragments of F-actin were diffusely distributed in the cytoplasm of most EGFP-expressing cells (Fig. 8C). In contrast, stress fibers in most SE-expressing cells were protected from staurosporine-induced collapse (Fig. 8D). Moreover, F-actin aggregation was detected in some SE-expressing cells (Fig. 8E). Cells were characterized according to whether they contained diffuse, filamentous, or aggregated F-actin. Actin in both untreated EGFP- and SE-expressing cells was filamentous. Staurosporine treatment increased the proportion of diffuse F-actin in EGFP-expressing cells, whereas ectopic expression of SE prevented the diffuse actin phenotype (Fig. 8F). These data indicate that SE expression counteracted the F-actin breakdown induced by staurosporine.

Discussion

SYNPO regulates α-actinin-dependent actin-bundling and formation of stress fibers in renal podocytes (Asanuma et al., 2005). Since F-actin is the major cytoskeletal component of neuronal dendritic spines (Fifkova and Delay, 1982; Matus et al., 1982), spine-specific localization of neuronal SYNPO (Mundel et al., 1997)

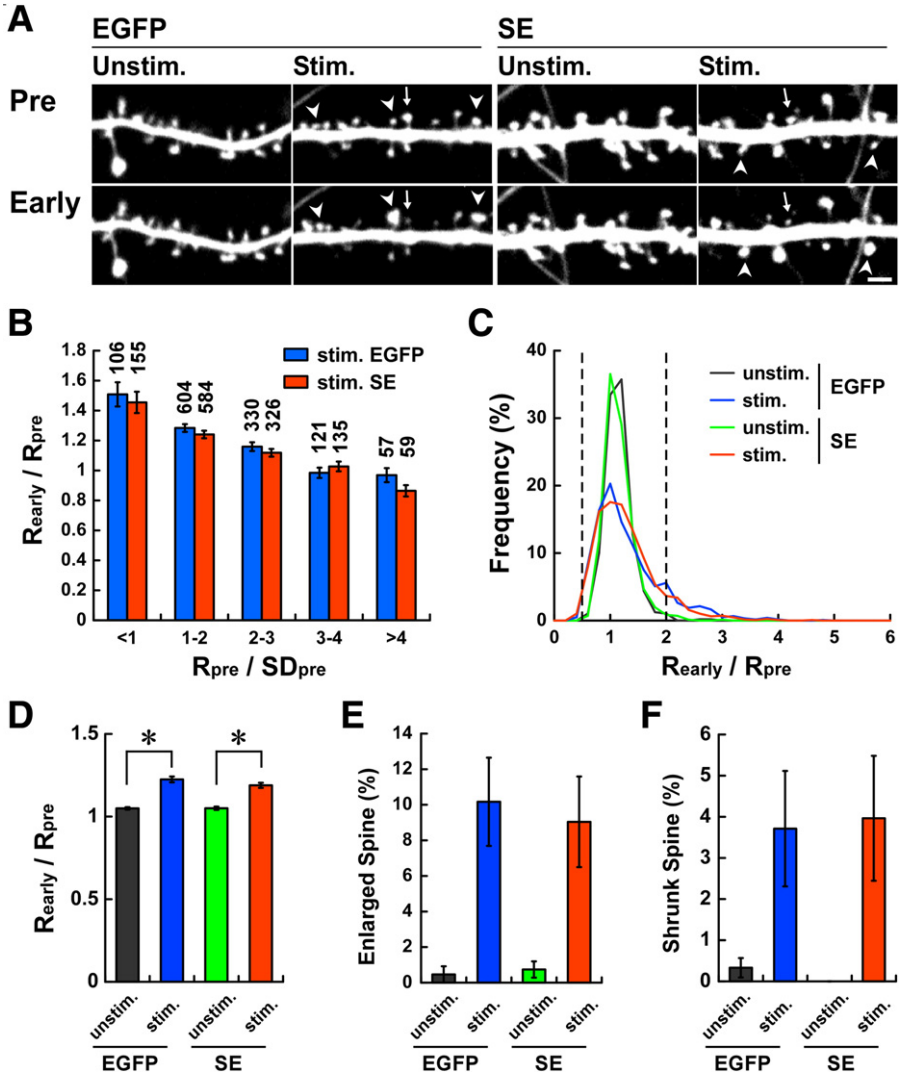

Fig. 5. Overexpression of SYNPO does not affect the evoked enlargement of spines in early stage. (A) Hippocampal cultures were co-transfected with DsRed2 and EGFP or SE on 9 DIV, and were imaged on 21-27 DIV. DsRed2 images of neurons co-expressing EGFP or SE were taken 15 min before the stimuli (Pre) and 15 min after the stimuli (Early). Arrowheads highlight spines that had at least doubled in size, while arrows indicate spines which were reduced in volume to less than half their original size. Scale bar, 2 μm. (B) Larger changes in size were observed in spines with initially smaller volumes. Average fold changes in DsRed2 fluorescence in the early stage relative to the pre-stimulus (R_{early}/R_{pre}) in spines, compared to R_{pre}, normalized by the standard deviation of R_{pre} (SD_{pre}) of each neuron so that comparisons between neurons could be made. The number of spines analyzed of each size is indicated above the columns. Spines with $R_{pre}/SD_{pre}<1$ show significantly larger R_{early}/R_{pre} than other spines. (C) Histogram of DsRed2 fluorescence changes in spines. Ratios of fluorescence intensities in the early phase (R_{early}) to that of pre-stimulus (R_{pre}) are shown on the horizontal axis. (D) Average ratio of R_{early} to R_{pre}. Asterisks indicate $p<0.001$. (E) Percentage of enlarged (more than two fold) spines in the early stage. (F) Percentage of reduced volume (less than half) spines in the early stage.

implies that it may be involved in a similar regulation of spine morphology. The present study, however, revealed that, in neurons, SYNPO is not involved in F-actin formation, because SYNPO overexpression (Fig. 4), as well as lack of expression (Deller et al., 2003), does not affect the number or size of spines. Instead, the present study showed that SYNPO overexpression persistently maintains NMDA receptor activation-dependent spine enlargement, which was transient in control neurons (Fig. 6). Additionally, SYNPO has a protective effect on F-actin that counteracts stress fiber disruption by staurosporine (Fig. 8). Thus, SYNPO is involved in F-actin formation in renal podocytes, while in neurons it maintains the activity-dependent increase in spine volume. Such differential roles of SYNPO in F-actin dynamics may be the result of the difference in SYNPO splice variants expressed in the brain and the kidney, since the C-terminal region of renal Synpo-long, which includes the α-actinin binding sites, is lacking in neuronal Synpo-short (Asanuma et al., 2005).

Pharmacological stimuli similar to ours induce LTP in hippocampal slices (Kopec et al., 2006; Otmakhov et al., 2004) and primary hippocampal neuron cultures (Lu et al., 2001). Spine volume is correlated with AMPA receptor currents (Matsuzaki et al., 2001), thereby providing a measure of morphological plasticity. High- and low-frequency stimuli cause growth and reduction of spine size, respectively (Okamoto et al., 2004). Although we did not confirm LTP induction electrophysiologically, our protocol pharmacologically activating synaptic NMDA receptors is also likely to induce LTP, because a sub-population of spines was enlarged or reduced in volume (Fig. 5). Enlarged spines in our experiments

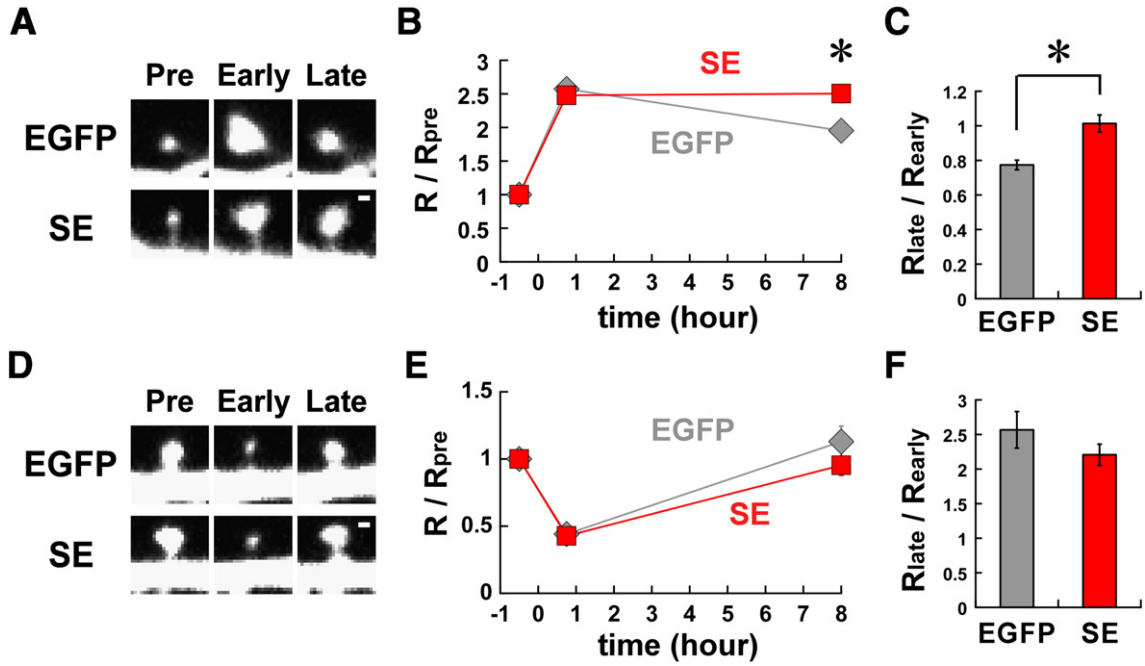

Fig. 6. Spines overexpressing SYNPO maintained their enlarged size in late stage. (A–C) Spines that have enlarged by more than two fold in the early stage (EGFP, 129 spines; SE, 107 spines). Note that the volume of the enlarged spines of SE-expressing neurons remained steady between the early and late stages, while the EGFP control spines decreased in size. Scale bar, 1 μm. (D–F) Spines that have undergone a two-fold reduction in size during the early stage (EGFP, 41 spines; SE, 46 spines). (A, D) Representative DsRed2 images of spines at the Pre, Early, and Late stages. (B, E) Average time course of DsRed2 fluorescence (R). (C) and (F) Average DsRed2 intensity ratio in the late stage relative to the early stage. Asterisks indicate a significant change ($p<0.001$).

would be those that received high frequency activity from presynaptic fibers, while low-frequency activity caused a reduction in spine volume. Furthermore, spine growth that did not last for 8 h in control neurons suggests that the morphological plasticity corresponding to E-LTP, not L-LTP, was evoked under our conditions. Expression of neuronal SYNPO increases during L-LTP induction (Yamazaki et al., 2001) and is required for L-LTP (Deller et al., 2003). L-LTP is accompanied by an increase in F-actin in the activated synaptic layer, and inhibition of actin polymerization impairs L-LTP (Fukazawa et al., 2003), suggesting that L-LTP involves the persistent maintenance of increased spine volume. Overexpression of SYNPO successfully transformed transient morphological plasticity to the persistent form in our experiments, suggesting that SYNPO-dependent maintenance of activity-dependent morphological changes may contribute to L-LTP. Examination of this requirement for SYNPO in L-LTP will be the subject of a future study, but RNAi of SYNPO did not affect spine size following application of the present (presumably E-LTP-evoking) stimulation protocol (data not shown). Future studies should include combining L-LTP evoking stimuli with SYNPO knockout or knockdown.

Our results indicate that SYNPO somehow protects F-actin from disruption (Fig. 8). Next, it will be important to study SYNPO function in L-LTP to clarify how SYNPO regulates spine volume. Several signaling pathways controlling SYNPO–F-actin interactions can be hypothesized. First, SYNPO may stabilize F-actin by blocking signals that induce actin disruption. SYNPO suppresses Rho degradation (Asanuma et al., 2006; Tashiro et al., 2000), and, consistent with a Rho-dependent mechanism, RhoB is activated in LTP (O'Kane et al., 2003, 2004). Secondly, SYNPO may alter the dynamic equilibrium of actin treadmilling. The turnover rate of F-actin in the spine is not homogeneous and is very slow near the neck of the spine, where SYNPO is localized (Honkura et al., 2008), suggesting that SYNPO may modulate the dynamic equilibrium between G- and F-actin. Thirdly, considering the roles of the cytoskeleton in intracellular transport, intraspine transport may be altered by increases in SYNPO-F-actin interactions, which may influence the distribution and composition of synaptic components such as NMDA receptors. Finally, we do not exclude the possibility that SYNPO stabilizes spine volume without a direct interaction with F-actin. Slice cultures from SYNPO knockout mice showed a substantial reduction in the amplitude and increase in the width of calcium transients (Drakew et al., 2007), which may be a consequence of the lack of spine apparatus in the knockout. These observations also suggest that SYNPO overexpression may alter calcium dynamics as well.

It will also be of interest to determine whether the actin stabilizing effect is specific to SYNPO among the many actin-associated proteins, such as cortactin, ABP, drebrin, and WAVE. However, to our knowledge SYNPO is the only protein among many actin-associated proteins that is upregulated during L-LTP. Therefore, we hypothesize that the stabilization of spine volume during late-phase is specific for SYNPO.

Experimental methods

Dentate gyrus LTP in unanesthetized freely moving animals

LTP experiments with freely moving rats were carried out as described previously (Fukazawa et al., 2003). To elicit LTP, high frequency stimulation (HFS) was delivered after establishing the baseline recording. The HFS consisted of four trains of stimuli at 15-min intertrain intervals. Each train consisted of 20 bursts of 30 pulses at 400 Hz, delivered at 5-s interburst intervals.

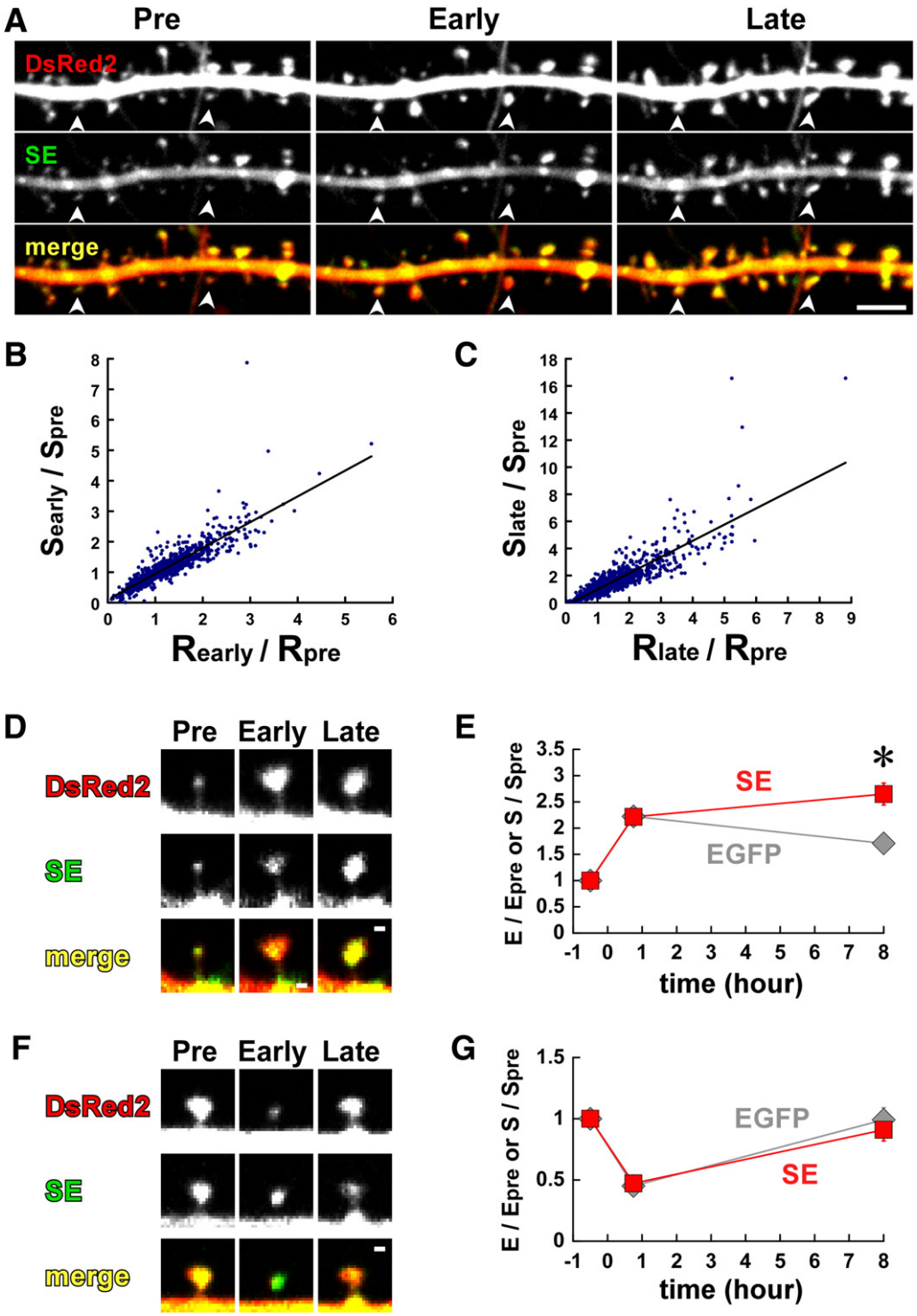

Fig. 7. SYNPO is recruited into enlarged spines in the late stage. (A) Fluorescence images of neurons expressing both DsRed2 (top panel and red in bottom panel) and SE (middle panel and green in bottom panel). Scale bar, 5 μm. (B, C) Correlation between fluorescence fold changes of SE (S) and DsRed2 (R) in individual spines. Fold changes during the early stage are expressed as R_{early}/R_{pre} and S_{early}/S_{pre} in (B), while R_{late}/R_{pre} and S_{late}/S_{pre} indicate the fold changes during the late stage in (C). (D, F) Examples of DsRed2 and SE images of spines which have enlarged (D) or lost volume (F) in the early stage. Scale bar, 1 μm. (E, G). The fold change in SE (S) and EGFP (E) fluorescence intensities in enlarged (E) and reduced volume (G) spines. Asterisks indicate a significant change ($p<0.001$).

In situ hybridization

In situ hybridization was carried out as described previously (Yamazaki et al., 2001). In brief, rat brains were frozen in crushed dry ice and frontal sections of 10 μm thickness were prepared. To prepare kidney specimens, rats were perfused with 4% paraformaldehyde. The kidneys were removed and fixed in 4% paraformaldehyde for 2 h, cryoprotected in phosphate-buffered saline (PBS) containing 25% sucrose for approximately 48 h,

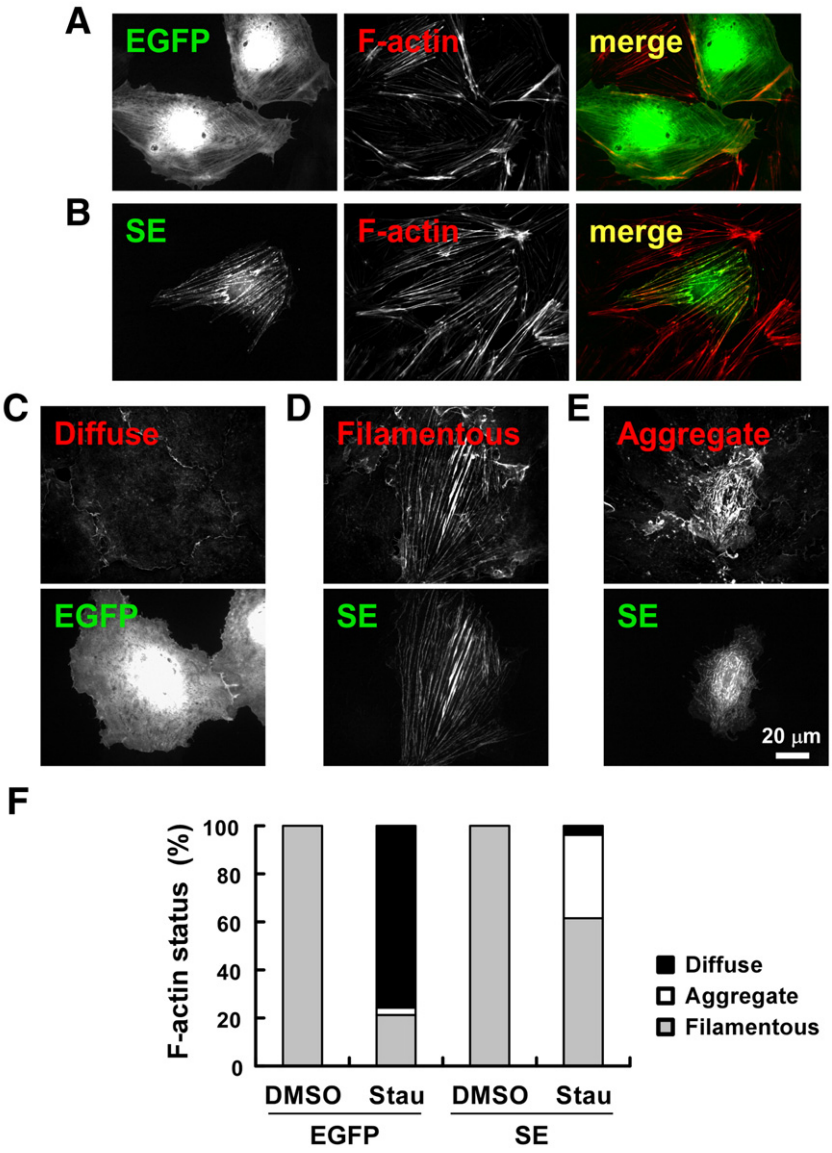

Fig. 8. Ectopic expression of SYNPO inhibited staurosporine-induced disruption of F-actin stress fibers in PtK2 cells. (A, B) PtK2 cells were transfected with EGFP (A) or SE (B), and stained with TRITC-phalloidin (F-actin). SE colocalized with stress fibers (B) while EGFP was distributed uniformly (A). (C–E) Most stress fibers in EGFP-expressing cells were disrupted with 100 nM staurosporine treatment for 20 min (C), while SE-expressing cells maintained filamentous and aggregated actin (D, E). (F) The percentage of cells containing diffuse, filamentous, or aggregated F-actin was estimated.

frozen in crushed dry ice and transverse sections of 10 μm thickness were cut. We used DIG-labeled cRNA probes for hybridization (probe 1: +396 to +1334, probe 2: +2110 to +2609, probe 3: +2287 to +2654) as indicated in Fig. 1A, where the adenine residue of the initiation codon of Synpo-short (probe 1 and 2) or Synpo-long (probe 3) was designated as +1. PCR products amplified with the following primers were inserted into plasmids for templates of these probes: probe 1, as in (Yamazaki et al., 2001); probe 2, 5′-GTGTGGAAACCTTCCTTCTGC-3′ and 5′-AAAATGTCCA-GAAGGCAGAGG-3′; probe 3, 5′-CTTCTGGCACGCAACATCAT-3′ and 5′-CCCCGAGGACAGATGTTGTA-3′.

Plasmid constructs

Plasmids encoding EGFP and SYNPO-EGFP (SE) were constructed by inserting EGFP from the pEGFP-N1 vector (BD Biosciences Clontech, Palo Alto, CA) into the pGL3-Basic vector (Promega, Madison, WI). The SE plasmid containing the sequence encoding rat Synpo-short was previously cloned in our laboratory (Yamazaki et al., 2001). We used the Δ13 domain of the Vesl-1 (Homer-1) promoter and the polyA region from Vesl-1S (Homer-1a) (1SpA) to drive expression of EGFP and SE in neurons (Niibori et al., 2007). A Myc-tagged SYNPO was also constructed in the pcDNA3.1 (−) vector (Invitrogen, Carlsbad, CA) containing a CMV promoter. The pDsRed2-N1 vector (BD Biosciences Clontech, Palo Alto, CA) was used to express DsRed2 uniformly in neurons so that spine volume could be measured.

Western blot analysis

Western blotting analysis was performed as described previously (Ohkawa et al., 2007) except that the Immobilon P (Millipore, Bedford, MA) after blocking was incubated with a rabbit anti-synaptopodin antibody (1:3000, SE-19, Sigma-Aldrich, St. Louis, MO) for 2 h and that a horseradish peroxidase-conjugated goat anti-rabbit IgG antibody (Jackson ImmunoResearch Laboratories, West Grove, PA) was used at 1:5000 for 2 h.

Primary cultures of hippocampal neurons

Hippocampi were dissected from Wistar rats on embryonic day 18 and dissociated using the Sumilon Nerve–Cell Dissociation kit (Sumitomo Bakelite, Tokyo, Japan). For low density culture, neurons were plated at a density of 1.0×10^4 cells/cm^2 on cover slips coated with 1 mg/ml poly-L-lysine (Sigma) in Dulbecco's modified Eagle's medium (DMEM) (Invitrogen) containing 5% horse serum and 5% fetal calf serum. After the neurons had attached, cover slips were transferred face down into a dish containing an astrocyte monolayer and maintained for 3 weeks in serum-free DMEM with N2 supplements, 1 mM sodium pyruvate, and 0.1% ovalbumin. For high density culture, neurons were suspended in MEM (Gibco BRL) supplemented with 5% horse serum, 5% fetal calf serum, 2 mM L-glutamine and 1 mM pyruvic acid. The dissociated cells were plated onto poly-L-lysine-coated glass cover slips using Flexiperm (Vivascience, Hanau, Germany) at a density of 4.2×10^4 cells/cm^2. On the first day in vitro (DIV), the medium was replaced with MEM containing a B27 supplement (Gibco BRL) and 0.5 mM L-glutamine. Neurons were transfected with 2–3 μg of DNA using Lipofectamine 2000 (Invitrogen) on 9 DIV, and imaged on 21–27 DIV.

Immunocytochemistry

Primary cultures of hippocampal neurons (21–27 DIV) or PtK2 cells (2 days after transfection) were fixed in 4% paraformaldehyde in 50 mM PBS at pH 7.4 for 30 min. Cells were permeabilized with 0.2% Triton X-100 in PBS for 5 min, and then incubated in PBS containing 5% goat serum and 0.1% Triton X-100 for 30 min at room temperature. Cells were incubated with a rabbit anti-synaptopodin antibody (1:3000, SE-19, Sigma) overnight at 4 °C. After washing with PBS, the cells were incubated with Alexa Fluor 488-conjugated goat anti-rabbit IgG (H+L) (1:1000, Molecular Probes, Eugene, OR), and/or TRITC-labeled phalloidin (0.1 μg/ml, Sigma) to stain F-actin, for 2 h at room temperature. ProLong Gold Antifade Reagent (Molecular Probes) was used to protect samples from bleaching. Fluorescence images were obtained using an LSM confocal laser scanning microscope (Carl Zeiss, Göttingen, Germany) through a 100× Plan-NeoFluor objective (NA 1.30, Carl Zeiss), or a CSU-22 spinning-disc confocal unit (Yokogawa Electric, Tokyo, Japan) coupled to an Axiovert 200M microscope through a 63× Plan-Apochromat objective (NA 1.4, Carl Zeiss).

Analysis of spine number and area

Stacked images of consecutive focal planes of 0.5 μm intervals (z-series sections) were reconstructed into a 2D projection image using the LSM Image Browser software (Carl Zeiss). EGFP fluorescence was measured and MetaMorph software (Universal Imaging Corporation, West Chester, PA) was used to calculate the number and area of mushroom-shaped and stubby-type spines. Spines from five dendrites 40 μm distal to the first branch point in each neuron were selected and regions of interest (ROIs) were manually outlined.

The relationship between spine size and endogenous SYNPO localization in high density cultures was estimated by measuring the spine projection area of EGFP-transfected cells after anti-SYNPO immunostaining (red). Spines were found in EGFP images and classified as SYNPO-expressing spines when the maximal intensity of the immunostained image (8 bit color) was saturated. Immunostaining signals outside of spines were taken from adjacent non-EGFP-expressing cells.

Time-lapse imaging

A cover slip was attached to the recording chamber and cells were perfused with artificial cerebrospinal fluid (ACSF) (in mM: 124 NaCl, 26 $NaHCO_3$, 1.25 NaH_2PO_4, 10 D-glucose, 2.5 KCl, 2.5 $CaCl_2$, 1.5 $MgCl_2$, and 1.0 mannitol) gassed with 5% CO_2 and 95% O_2 at 30 °C and a flow rate of 0.5 ml/min. To activate synaptic NMDA receptors, Mg^{2+}-free ACSF containing 10 μM glycine and 3 μM picrotoxin, was applied 3 times for 5 min at 5 min intervals. Transfected neurons were identified under epifluorescence illumination. Proximal dendritic regions up to 500 μm away from the first branch were chosen for data acquisition. Fluorescence imaging was performed using an Axiovert 200M inverted microscope (Carl Zeiss) equipped with a CSU-22 laser confocal unit (Yokogawa Electric) under the control of MetaMorph software (Universal Imaging). An air-cooled Ar/Kr laser (Melles Griot, Carlsbad, CA) was fiber-optically coupled to the spinning head and filter wheels were selected for illumination at 488 nm or 568 nm. An Orca-ER CCD camera (Hamamatsu Photonics, Hamamatsu, Japan) was used to take images through a 63× Plan-Apochromat oil-immersion objective (NA 1.4, Carl Zeiss). Images were acquired −30, −15, 0, 15, 30, 45, 450, 465, 480 min after the stimulus. For each time point, images at 11 focal planes with an interval of 0.3 μm between planes were captured to generate a stacked image.

Quantitative analysis of spine volume, SE, and EGFP in spines

A 3D-reconstructed image was made from the stacked images acquired at each time point. Horizontal positions of the reconstruction images were aligned among time points. Spines were identified by DsRed2 fluorescence, and ROIs were manually positioned to fully cover each spine. Any spine that appeared, disappeared, overlapped with dendrites, or moved out of the focal plane was excluded. Approximately, 80–250 mushroom-shaped and stubby spines were identified in each image. Integrated fluorescence intensities of red (DsRed2) and green (SE or EGFP) channels in the ROIs were calculated and the background intensity was subtracted. Because the expression levels of DsRed2, SE, and EGFP differed from neuron to neuron, the fold changes relative to the average of the pre-stimulus images (taken at −30, −15 and 0 min) were used for comparison. The early-stage change was defined as the average fold change of images captured at 15, 30 and 45 min after stimulation, while the late-stage change was measured as the average fold change of images captured at 450, 465, and 480 min. The fold change in DsRed2 fluorescence was considered a relative measure of volume change.

PtK2 cells and staurosporine treatment

PtK2 cells (American Type Culture Collection, Rockville, MD), derived from the kidney of a male rat kangaroo, were cultured in MEM supplemented with 10% fetal calf serum, 2 mM L-glutamine, 1% nonessential amino acids, 1 mM sodium pyruvate and 10 mg/ml gentamycin sulfate (Gibco BRL, Paisley, UK). For transfection, cells were seeded on 4-well polyethylenimine-coated BD Falcon culture slides (BD Biosciences, Bedford, MA) at a density of 3.0×10^4 cells/well. One day after plating, cells were transfected with 1 μg of DNA per well using Lipofectamine 2000 (Invitrogen). Two days after transfection, the cells were treated with either 100 nM staurosporine (Sigma) in 0.1% dimethylsulfoxide (DMSO) or 0.1% DMSO alone as a negative control.

Quantitative analysis of F-actin in PtK2 cells

Stacked images of 5 consecutive focal planes (z-series sections) were captured and a 2D-projection image was reconstructed using MetaMorph software. Transfected cells were identified by EGFP fluorescence and ROIs were manually positioned to fully cover each transfected cell. The three types of F-actin arrangement were determined based on the phalloidin staining pattern. When a cell did not contain TRITC-labeled filamentous structures, the cell was considered stress fiber-free and classified as 'diffuse'. The 'filamentous' class of cells had TRITC-labeled filaments but no aggregates, while the 'aggregated' class contained both actin filaments and aggregates in the cell.

Acknowledgments

We would like to thank Dr. Y. Saitoh for providing the LTP-induced rat brains for *in situ* hybridization experiments, Dr. Y. Shoji-Kasai for providing the low density cultures of hippocampal neurons, Ms. F. Ozawa for her instruction on culture methods, and

Dr. N. Ohkawa for advice on *in situ* hybridization experiments. This work was supported by the Special Coordinate Funds for Promoting Science and Technology from MEXT of the Japanese Government (K.I.), and supported in part by Grants-in-Aid for Scientific Research on Priority Areas <Neural Circuit Project>, <Advanced Brain Science Project>, and <Molecular Brain Science>, from MEXT of the Japanese Government (K.I.).

References

Asanuma, K., Kim, K., Oh, J., Giardino, L., Chabanis, S., Faul, C., Reiser, J., Mundel, P., 2005. Synaptopodin regulates the actin-bundling activity of alpha-actinin in an isoform-specific manner. J. Clin. Invest. 115, 1188–1198.

Asanuma, K., Yanagida-Asanuma, E., Faul, C., Tomino, Y., Kim, K., Mundel, P., 2006. Synaptopodin orchestrates actin organization and cell motility via regulation of RhoA signalling. Nat. Cell Biol. 8, 485–491.

Deller, T., Korte, M., Chabanis, S., Drakew, A., Schwegler, H., Stefani, G.G., Zuniga, A., Schwarz, K., Bonhoeffer, T., Zeller, R., Frotscher, M., Mundel, P., 2003. Synaptopodin-deficient mice lack a spine apparatus and show deficits in synaptic plasticity. Proc. Natl. Acad. Sci. U. S. A. 100, 10494–10499.

Deller, T., Merten, T., Roth, S.U., Mundel, P., Frotscher, M., 2000. Actin-associated protein synaptopodin in the rat hippocampal formation: localization in the spine neck and close association with the spine apparatus of principal neurons. J. Comp. Neurol. 418, 164–181.

Drakew, A., Klatt, N., Tippmann, A., Hoffmann, T., Vida, I., Deller, T., Frotscher, M., 2007. The spine apparatus shapes calcium transients in dendritic spines. Two-photon laser scanning microscopy-based calcium imaging at individual synapses in organotypic slice cultures. Society for Neuroscience 470.12.

Fifkova, E., Delay, R.J., 1982. Cytoplasmic actin in neuronal processes as a possible mediator of synaptic plasticity. J. Cell Biol. 95, 345–350.

Fukazawa, Y., Saitoh, Y., Ozawa, F., Ohta, Y., Mizuno, K., Inokuchi, K., 2003. Hippocampal LTP is accompanied by enhanced F-actin content within the dendritic spine that is essential for late LTP maintenance in vivo. Neuron 38, 447–460.

Hardingham, G.E., Fukunaga, Y., Bading, H., 2002. Extrasynaptic NMDARs oppose synaptic NMDARs by triggering CREB shut-off and cell death pathways. Nat. Neurosci. 5, 405–414.

Hedberg, K.K., Birrell, G.B., Habliston, D.L., Griffith, O.H., 1990. Staurosporine induces dissolution of microfilament bundles by a protein kinase C-independent pathway. Exp. Cell Res. 188, 199–208.

Honkura, N., Matsuzaki, M., Noguchi, J., Ellis-Davies, G.C., Kasai, H., 2008. The subspine organization of actin fibers regulates the structure and plasticity of dendritic spines. Neuron 57, 719–729.

Inokuchi, K., Kato, A., Hiraia, K., Hishinuma, F., Inoue, M., Ozawa, F., 1996a. Increase in activin beta A mRNA in rat hippocampus during long-term potentiation. FEBS Lett. 382, 48–52.

Inokuchi, K., Murayama, A., Ozawa, F., 1996b. mRNA differential display reveals Krox-20 as a neural plasticity-regulated gene in the rat hippocampus. Biochem. Biophys. Res. Commun. 221, 430–436.

Kato, A., Ozawa, F., Saitoh, Y., Hirai, K., Inokuchi, K., 1997. vesl, a gene encoding VASP/Ena family related protein, is upregulated during seizure, long-term potentiation and synaptogenesis. FEBS Lett. 412, 183–189.

Kopec, C.D., Li, B., Wei, W., Boehm, J., Malinow, R., 2006. Glutamate receptor exocytosis and spine enlargement during chemically induced long-term potentiation. J. Neurosci. 26, 2000–2009.

Lu, W., Man, H., Ju, W., Trimble, W.S., MacDonald, J.F., Wang, Y.T., 2001. Activation of synaptic NMDA receptors induces membrane insertion of new AMPA receptors and LTP in cultured hippocampal neurons. Neuron 29, 243–254.

Matsuo, R., Kato, A., Sakaki, Y., Inokuchi, K., 1998. Cataloging altered gene expression during rat hippocampal long-term potentiation by means of differential display. Neurosci. Lett. 244, 173–176.

Matsuo, R., Murayama, A., Saitoh, Y., Sakaki, Y., Inokuchi, K., 2000. Identification and cataloging of genes induced by long-lasting long-term potentiation in awake rats. J. Neurochem. 74, 2239–2249.

Matsuzaki, M., Ellis-Davies, G.C., Nemoto, T., Miyashita, Y., Iino, M., Kasai, H., 2001. Dendritic spine geometry is critical for AMPA receptor expression in hippocampal CA1 pyramidal neurons. Nat. Neurosci. 4, 1086–1092.

Matsuzaki, M., Honkura, N., Ellis-Davies, G.C., Kasai, H., 2004. Structural basis of long-term potentiation in single dendritic spines. Nature 429, 761–766.

Matus, A., Ackermann, M., Pehling, G., Byers, H.R., Fujiwara, K., 1982. High actin concentrations in brain dendritic spines and postsynaptic densities. Proc. Natl. Acad. Sci. U. S. A. 79, 7590–7594.

Mundel, P., Heid, H.W., Mundel, T.M., Kruger, M., Reiser, J., Kriz, W., 1997. Synaptopodin: an actin-associated protein in telencephalic dendrites and renal podocytes. J. Cell Biol. 139, 193–204.

Niibori, Y., Hayashi, F., Hirai, K., Matsui, M., Inokuchi, K., 2007. Alternative poly(A) site-selection regulates the production of alternatively spliced vesl-1/homer1 isoforms that encode postsynaptic scaffolding proteins. Neurosci. Res. 57, 399–410.

O'Kane, E.M., Stone, T.W., Morris, B.J., 2003. Activation of Rho GTPases by synaptic transmission in the hippocampus. J. Neurochem. 87, 1309–1312.

O'Kane, E.M., Stone, T.W., Morris, B.J., 2004. Increased long-term potentiation in the CA1 region of rat hippocampus via modulation of GTPase signalling or inhibition of Rho kinase. Neuropharmacology 46, 879–887.

Okamoto, K., Nagai, T., Miyawaki, A., Hayashi, Y., 2004. Rapid and persistent modulation of actin dynamics regulates postsynaptic reorganization underlying bidirectional plasticity. Nat. Neurosci. 7, 1104–1112.

Ohkawa, N., Fujitani, K., Tokunaga, E., Furuya, S., Inokuchi, K., 2007. The microtubule destabilizer stathmin mediates the development of dendritic arbors in neuronal cells. J. Cell Sci. 120, 1447–1456.

Otmakhov, N., Tao-Cheng, J.H., Carpenter, S., Asrican, B., Dosemeci, A., Reese, T.S., Lisman, J., 2004. Persistent accumulation of calcium/calmodulin-dependent protein kinase II in dendritic spines after induction of NMDA receptor-dependent chemical long-term potentiation. J. Neurosci. 24, 9324–9331.

Spacek, J., Harris, K.M., 1997. Three-dimensional organization of smooth endoplasmic reticulum in hippocampal CA1 dendrites and dendritic spines of the immature and mature rat. J. Neurosci. 17, 190–203.

Tashiro, A., Minden, A., Yuste, R., 2000. Regulation of dendritic spine morphology by the rho family of small GTPases: antagonistic roles of Rac and Rho. Cereb. Cortex 10, 927–938.

Yamazaki, M., Matsuo, R., Fukazawa, Y., Ozawa, F., Inokuchi, K., 2001. Regulated expression of an actin-associated protein, synaptopodin, during long-term potentiation. J. Neurochem. 79, 192–199.